Volume XCIV, No. 2, May 2024

Proceedings of the Danish Society for Structural Science and Engineering

Published by

Danish Society for Structural Science and Engineering

Merle van Logtestijn, Amalie Konrad Lassen, Lars German Hagsten: *Experimental study of circular point foundations with minimal reinforcement subjected by distributed load*……..……25-43

COPENHAGEN 2024

ISSN 1601-6548 (online)

PROCEEDINGS OF THE DANISH SOCIETY FOR STRUCTURAL SCIENCE AND ENGINEERING
Edited and published by the Danish Society for Structural Science and Engineering
Volume 94, No. 2, 2024.

Experimental study of circular point foundations with minimal reinforcement subjected by distributed load

Merle van Logtestijn[1]
Amalie Konrad Lassen[2]
Lars German Hagsten[3]

Introduction

As global population growth and urbanization accelerate, the demand for construction is rising rapidly, leading to increased consumption of resources such as concrete and steel. This presents significant environmental and economic challenges. According to the United Nations Environment Programme [6], the construction sector accounts for up to 40% of the world's raw material consumption and generates around 35% of global CO_2 emissions. Point foundations, which make up a substantial portion of constructions, contribute significantly to the overall resource demand in the building industry.

To alleviate the pressure on resources and reduce environmental impact, there is a need for optimized design that can decrease the usage of resources without compromising structural safety or performance. The experiment presented in this article is inspired by a new theory developed by Lars German Hagsten [1], which introduces an optimized reinforcement design for point foundations. This has the potential to reduce material consumption, CO_2 emissions, and costs, making it a crucial contribution to the future of sustainable construction practices.

Additionally, this approach can offer significant benefits for existing structures. During renovation or repurposing, where increased loads are introduced or requirements have been tightened, Hagsten's theory may allow for verification that the foundation’s capacity is sufficient, even with a reduced amount of reinforcement. This could eliminate the need for extensive foundation strengthening, saving resources and reducing the environmental and economic impact of refurbishment projects.

This article presents an experimental study conducted at Aarhus University, where six point foundations were subjected to compressive testing. As previously mentioned, the inspiration for this experiment is drawn from Hagsten’s theory, where one of the key parameters in his derivation is the distribution of the load. Therefore, this parameter has been closely examined, and the foundations were divided into two test groups, each with a different load distribution. Apart from this variation, the foundations were designed identically, with the aim of ensuring that failure due to the bending moment would be the governing design criterion.

[1] Student at Aarhus University, Value Engineering ApS,
[2] Student at Aarhus University, Aqvila A/S
[3] Aarhus University, Value Engineering ApS

The objective of the experiment is to test the minimal reinforcement requirements, wherefore the foundations are reinforced just below the minimum requirements as specified in [2], while still expecting a ductile failure. Following Hagsten's approach, the reinforcement was not bent upwards at the edges, allowing the reinforcement capacity to approach zero here.

In addition to presenting the experimental results, this article will analyze the practical findings with theory. The study will place the experiments into perspective with both L.G. Hagsten and K.W. Johansen [3][4]. Furthermore, it will compare the observed effects of the load distribution and the reduction in reinforcement capacity towards the foundation edges with Hagsten's derivation.

1. Experimental design

One of the objectives of the experiment is to examine the impact of the area over which the load is distributed. Accordingly, the specimens have been divided into two groups, with the only variable factor being the extent of the distributed load. A total of eight specimens are grouped as shown in Figure 1. Specimens subjected to a distributed load of Ø250 are assigned odd numbers, while those with a distributed load of Ø150 are assigned even numbers.

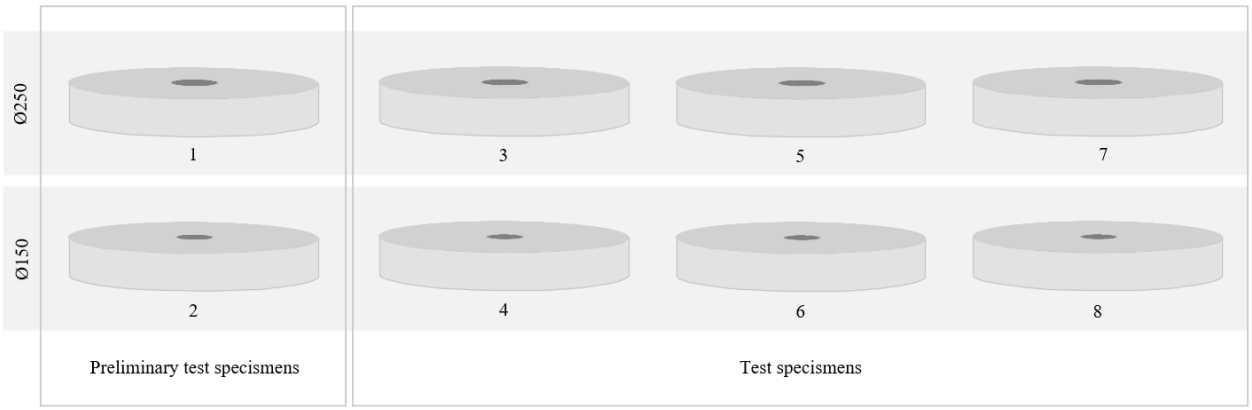

Figure 1 - Grouping and numbering of specimens

As shown in the figure above, 1 of 4 specimens in each group will act as a preliminary test specimen. In that way it is possible to adjust the experiment prior obtaining essential data from the 6 test specimens.

1.1 Design conditions and limits

The experiment was conducted at Aarhus University's BÆR-LAB in Navitas, where the actuator has an upper limit of 360 kN. Furthermore, it had to be placed on a beam with a maximum spacing of 2 meters. This sets the limit for the maximum applied load as well as geometric boundaries.

Furthermore, the point foundations were precasted at Industri Beton A/S in Perstrup, Denmark. The standard mix of concrete here is C45 with Y-steel as reinforcement, which forms the basis for the material strengths. Please note that mean values of the strengths are used throughout the study.

1.2 Experimental setup

The experimental setup is shown in Figure 2 and consists of three main components: (1) Load system, (2) Test specimen and (3) Support system. The following subsections will delve into each of these three in the respective order.

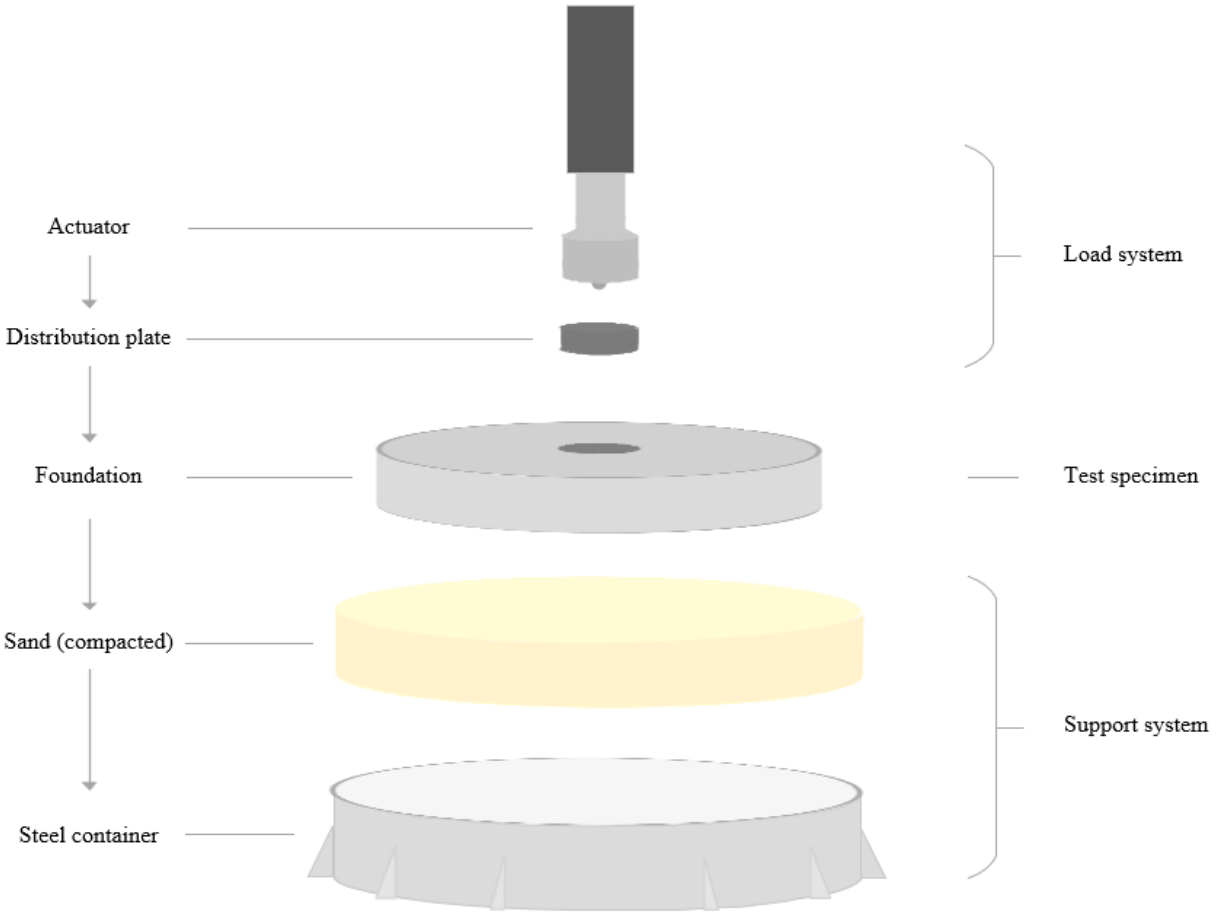

Figure 2 - Experimental setup

1.2.1 Load system

To ensure optimal load distribution, the actuator was equipped with a steel ball at its end, which fitted into a groove on the underlying distribution plate. The distribution plates had diameters of 150 mm and 250 mm, respectively, and a height of 100 mm, designed to ensure effective pressure distribution.

The actuator loaded the specimens 2 mm pr. min. This resulted in a test duration of approximately 15 minutes. The test stopped when the distributed plate loosened from the foundation. For further information on the actuator please see [7].

1.2.2 Test specimen

The foundations were utilized to 164% compared to the minimum requirements according to DS/EN 1992, as shown in the calculation below Figure 3. A ductile failure is still expected. The geometry was designed to accommodate the constraints outlined in section 1.1 and to prevent failure due to punching shear, which will be further elaborated upon in section 3.3. At the top of the foundation, a bearing plate was embedded to ensure uniform distribution of the contact pressure from the distribution plate.

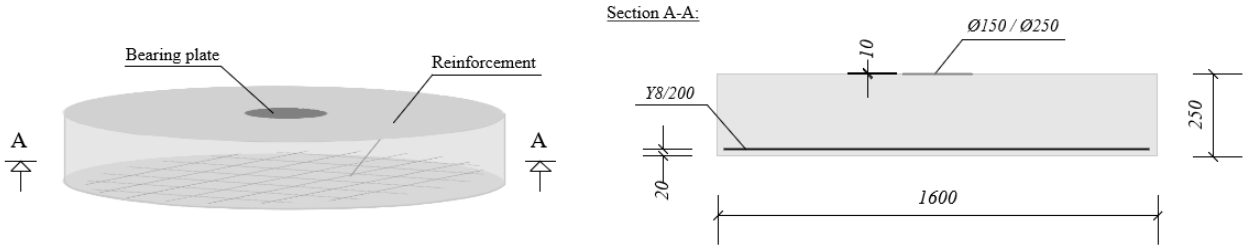

Figure 3 - Foundation design

Minimal reinforcement according to [2] 9.2.1.1:

Assuming: f_{ctm} = 4,23 MPa ([2] Table 3.1), f_t = 594 MPa ([2] Table C.1) and d = 250 mm – 20 mm – 8 mm = 222 mm.

$$A_{s.min} = \max\begin{cases} 0{,}26 \cdot \dfrac{f_{ctm}}{f_t} \cdot d \\ 0{,}0013 \cdot d \end{cases} = 411\ mm^2/m$$

Note that increased strengths have been used for both concrete and reinforcement, based on mean values.

Designed reinforcement:

Provided that: $ø$ = 8 mm and a = 200 mm.

$$A_s = \frac{\pi}{4} \cdot ø^2 \cdot \frac{1\ m}{a} = 251\ mm^2/m$$

Utilization:

$$\frac{A_{s.min}}{A_s} = 164\ \%$$

As it is mentioned the foundations are designed below minimal reinforcement. Still, a ductile failure is expected.

1.2.3 Support system

The foundations were supported by compacted sand enclosed in a steel container to strive for an evenly distributed reaction. The steel container was designed to ensure to horizontal displacements. Its dimensions are shown below.

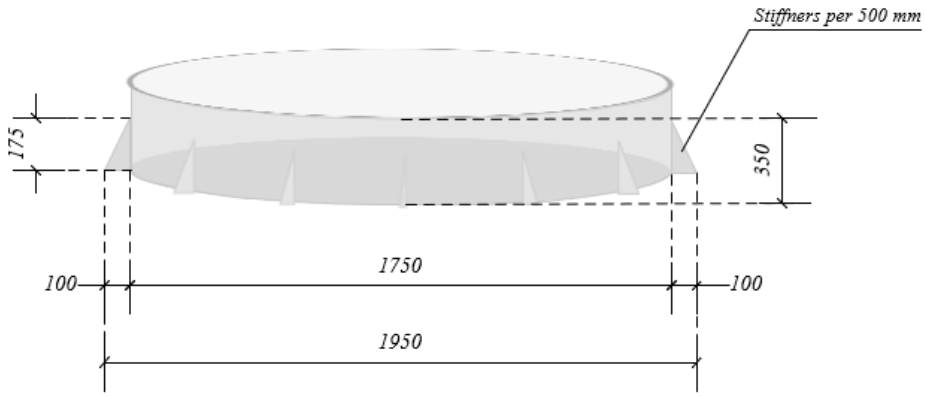

Figure 4 - Design of steel container

As the preliminary test specimens were subjected to load, it was seen that the foundations did not reach failure when subjected to the actuator's maximum capacity. Therefore, a pocket got introduced. This reduced the area of the distributed reaction weaking the support system. Through iterative testing of pocket sizes with the preliminary test specimens, it was found that a pocket of a diameter 1150 mm was sufficient for both specimen groups to reach failure. The pocket was made with a depth of 100 mm for all specimens.

To minimize variable factors a protocol was made upon the experiment to secure an as evenly as possible compacting of sand as well as excavating the pocket throughout the experiments. First, the sand was compacted, after which the footing was excavated. See Figure 5

Figure 5 – Steel container with compacted sand excavated for the pocket.

1.3 Data collection

The actuator measures and stores its displacement, while it loads the specimen. This data is essential to make the stress strain curves for each of the specimens. Additionally, several distance meters were placed on both the foundation and the steel container. This was ensured by placing three columns around the setup of which each were equipped with three distance meters. The placement of the distance meters follows Figure 6.

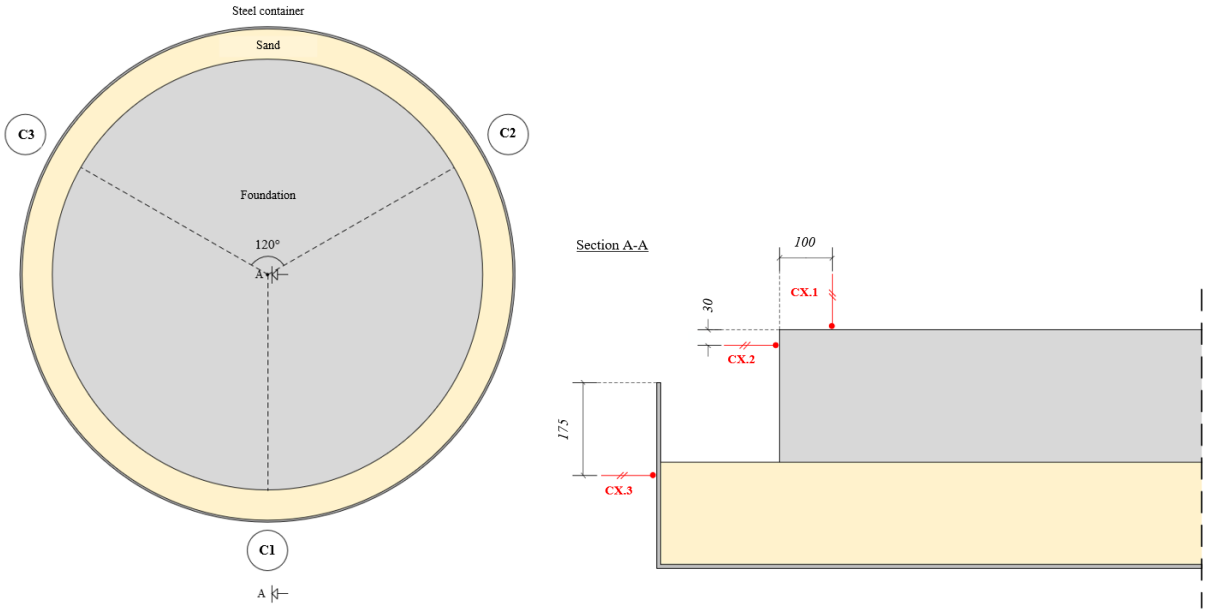

Figure 6 - Placement and notation of distance meters

As the horizontal distance meters, CX.2 and CX.3, did not measure significant displacements, this data will not be elaborated on in this study.

Finally, a distance meter was placed on top of the beam supporting the actuator to measure its counter displacement when loading the specimens.

1.4 Experimental setup in pictures

Pictures from the experimental setup are shown below.

Figure 7 - Experimental setup, pictures
a) Overall setup b) Load distribution c) Placement of distance meters

2. Results

First, the stress-strain curves obtained from the experiment will be presented. Next, the influence of the pocket will be incorporated, followed by an analysis of the foundation's load when reaching failure. Finally, an overview of the cracks will be shown.

2.1 Stress-strain curves

As mentioned in section 1.3 data for the stress-strain curve is obtained by the actuator. When the curves where developed it was seen that the elastic area didn't seem as linear as expected. Furthermore, it was seen that the displacement measured from CX.1 (see Figure 6) was large at the beginning of the tests. Subtracting this displacement from the stress-strain curve resulted in a far more linear curve for the elastic area. This was performed throughout the specimens, referring to the original data as the 'raw data curve' and the adjusted data as the 'corrected data curve.' This paper will only present the corrected data curves.

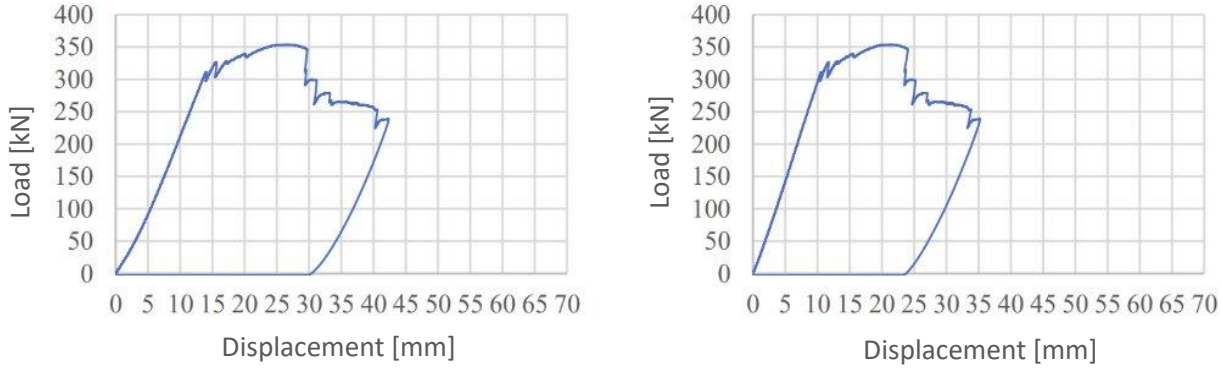

Figure 8 - Stress strain curve, example
a) Raw data curve b) Corrected data curve

2.1.1 Presenting the stress-strain curves

The stress-strain curves are gathered in the graph below. With blue nuances being the specimen group with a distributed load of Ø250 and green nuances the ones with Ø150.

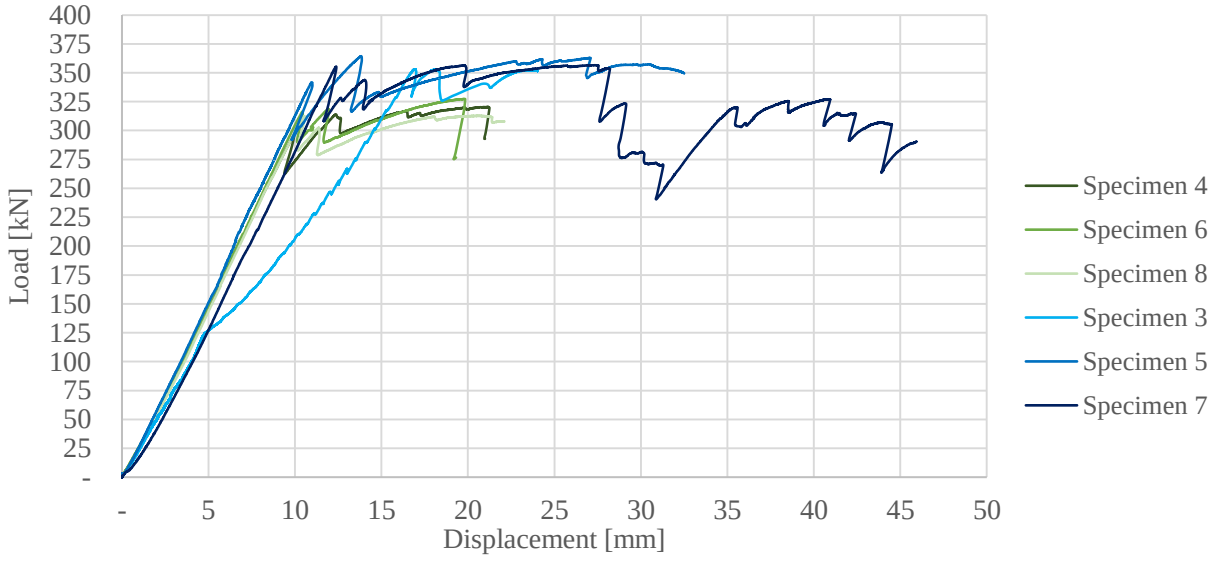

Figure 9 - Stress-strain curves gathered

As it was expected the failure was ductile. The test specimens with larger distributed load area obtained more ductility.

Below the mean value of each specimen group is presented.

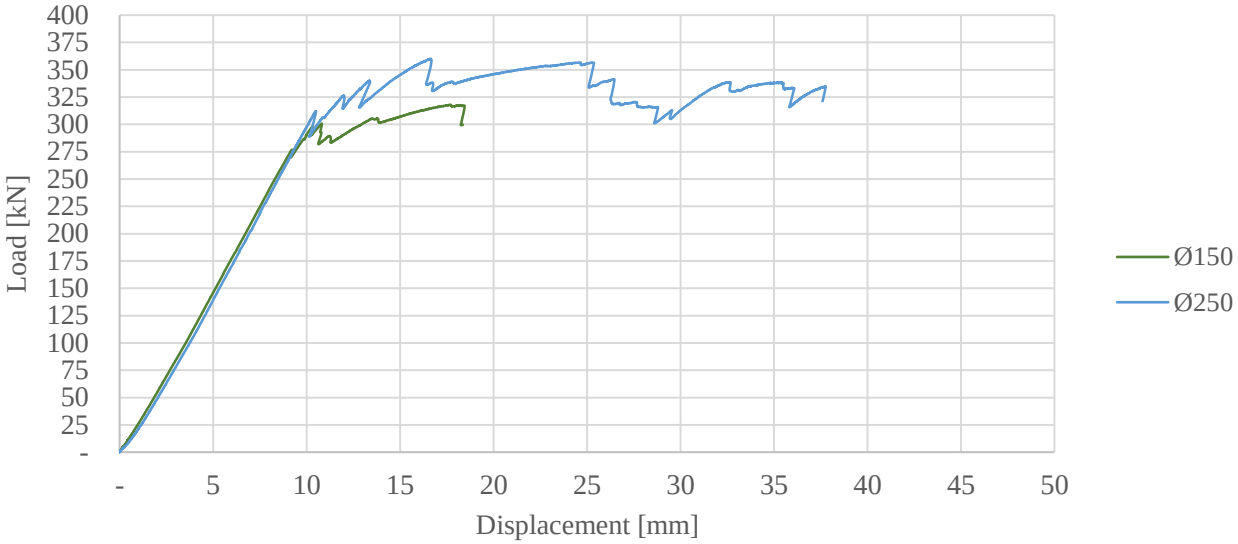

Figure 10 - Mean stress-strain curves

2.1.2 Measured data from the stress-strain curves

From the stress-strain curves in Figure 9 following loads when failure have been obtained.

Ø150	
Specimen number	Failure load [kN]
4	320
6	327
8	307
Avg.	318

Ø250	
Specimen number	Failure load [kN]
3	352
5	362
7	356
Avg.	357

Figure 11 – Measured failure load

2.2 Support conditions and its influences

Generally, the experiments show that the support conditions change for both specimen groups as the sand moves inwards when the foundation is subjected to load. Foundations with a load distribution of Ø250 exhibit a significantly greater change compared to those with Ø150. The data has been gathered and a mean value for the movements can be seen in Figure 12.

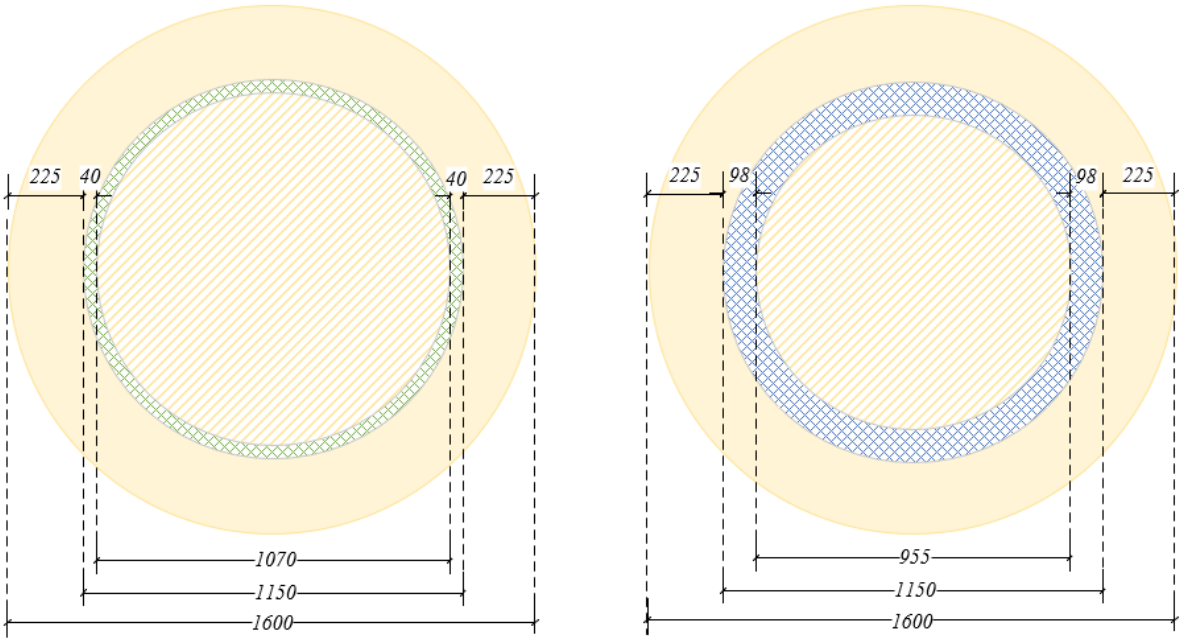

Figure 12 - Support conditions measured before and after testing
a) Specimen group, Ø150 b) Specimen group, Ø250

2.2.1 Load increment due to the pocket

Using the upper bound solution after K.W. Johansen [3][4] and further investigated by L.G. Hagsten [1] the pocket's influence has been derived from the failure mechanisms as shown in Figure 13. The notation follows [1] with an additional measurement for the pocket's diameter, R_2.

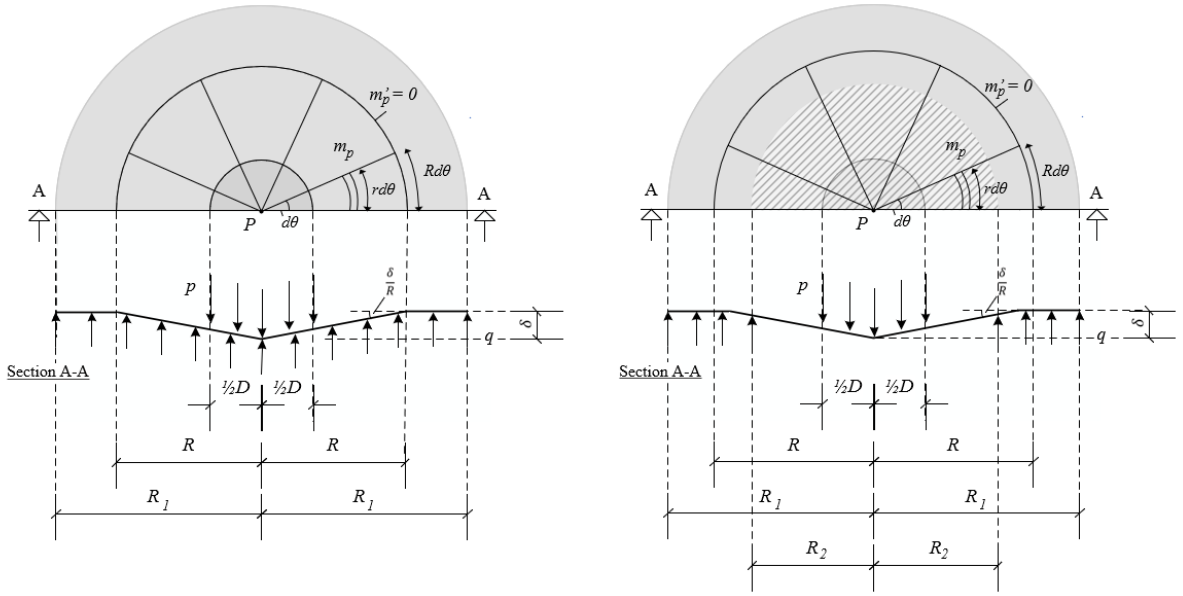

Figure 13 - Pocket influent on failure mechanism
a) Without pocket b) With pocket

With an example of a load equal to 350 kN a visualization of the increment due to pocket with is is seen below.

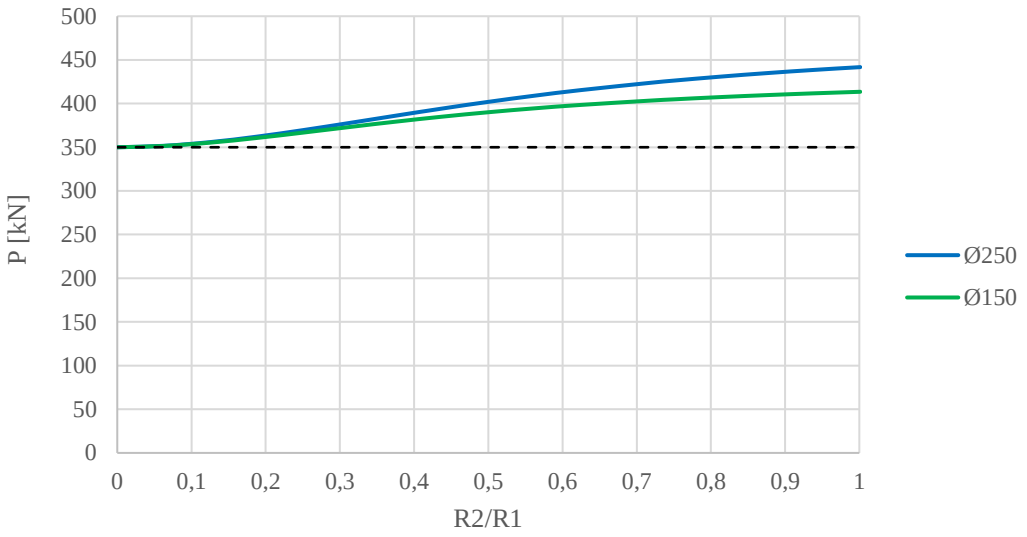

Figure 14 - Increment of load when the pocket increases

E.g. when implementing a pocket size of 1150 mm, it will correspond to increasing the load with 15,3% for Ø150 and 21,1% for Ø250.

For a deeper understanding of this calculation please see Appendix A.

2.2.2 Load of failure, pocket incorporated

The table below shows the load failure of which the pocket has been incorporated according to the method just presented. It was decided to use the size of the measured pocket after the test was completed, where the sand had shifted toward the center. This is because it represents the most accurate support condition, as the foundation settled quickly and before failure.

Ø150	
Specimen number	Failure load [kN]
4	367
6	375
8	351
Avg.	364

Ø250	
Specimen number	Failure load [kN]
3	421
5	423
7	423
Avg.	422

Figure 15 - Failure load with influence of the pocket incorporated

2.3 Cracks

The cracks where numbered respectively as they occurred.

Ø150	*Ø250*
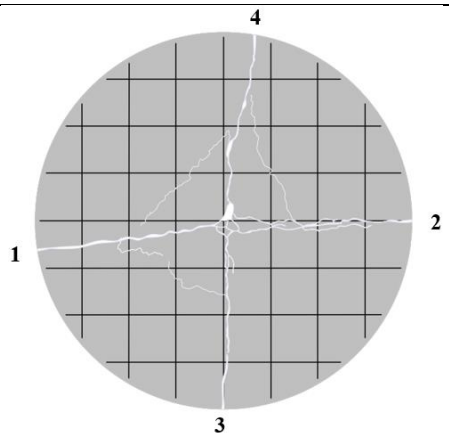 Specimen 4	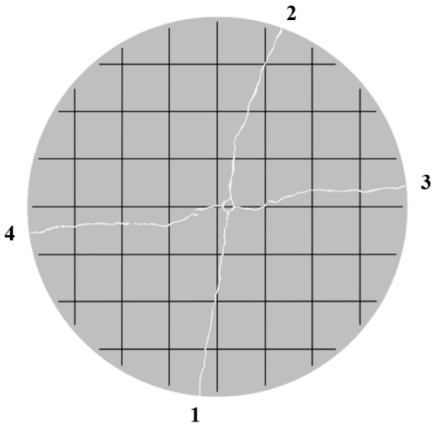 Specimen 3
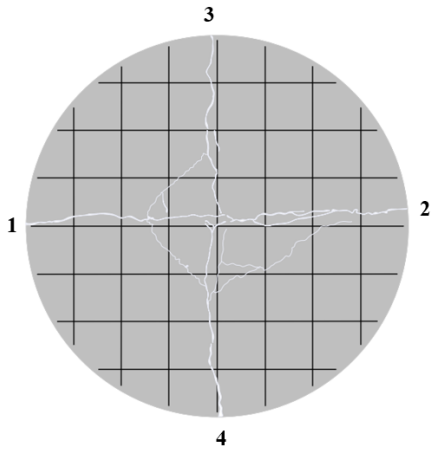 Specimen 6	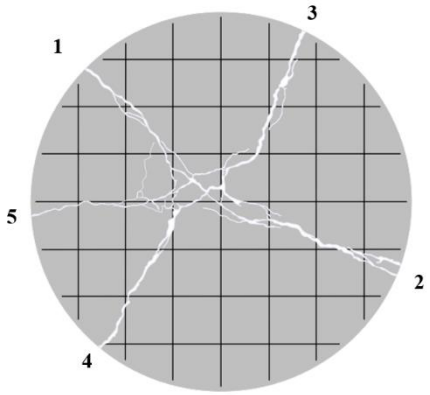 Specimen 5
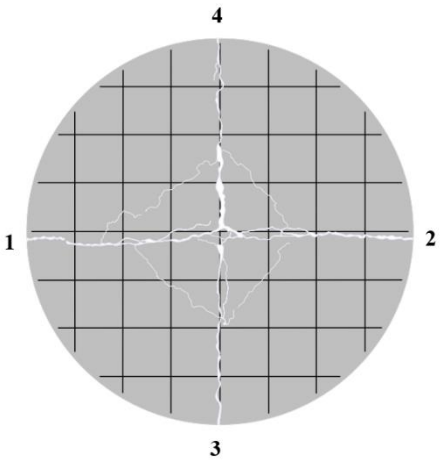 Specimen 8	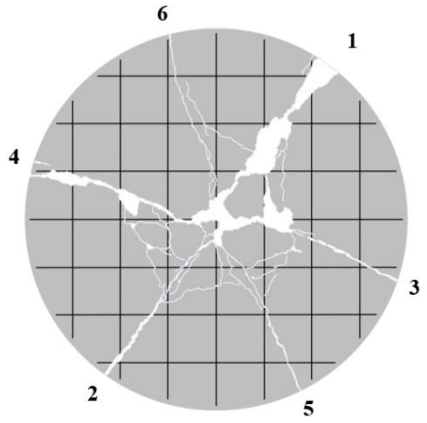 Specimen 7

3. Data analyze and discussion

3.1 Comparing data with theory for bending moment

The data will be compared with K.W. Johansen's upper bound solution [3][4] and L.G. Hagsten's lower bound solution [1]. It was discussed whether is should be compared to M.P. Nielsen as well, but this theory suggests a negative bending moment, which is not compatible with the reinforcement design studied in this paper.

3.1.1 Bending capacity

Parameters for the foundation is as described in section 1.2.2. Strength parameters follow mean values given by [2] Table 3.1, f_{cm} = 53 MPa, and table C.1, f_t = 594 MPa. Both are calculated with a partial factor γ_i = 1,0.

The capacity is calculated according to [5] section 5.4.1.

$$x = \frac{f_t \cdot A_s}{\eta \cdot f_{cm} \cdot \lambda \cdot b} = 3{,}52\ mm$$

As $\lambda = 0{,}8$ and $\eta = 1{,}0$ [5] Table 5.17 calculated pr meter: b = 1,0 m.

$$m_{Rd} = f_t \cdot A_s \cdot z = 32{,}9\ kNm\ /m$$

3.1.2 Load capacity according to K.W. Johansen

Calculation according to [3][4].

$$m_p = \frac{P}{2\pi}$$

Load capacity:

$$P_{max.KWJ} = m_{Rd} \cdot 2\pi = 207\ kN$$

3.1.3 Load capacity according to L.G. Hagsten

Notation and calculation according to [1].

$$m_\theta = m_r = \frac{P}{2\pi} \cdot \left(1 - \sqrt[3]{\frac{D^2}{4 \cdot {R_1}^2}}\right)$$

Load capacity:

$$P_{max.LGH.Ø150} = m_{Rd} \cdot \frac{2\pi}{\left(1 - \sqrt[3]{\frac{{D_{Ø150}}^2}{4 \cdot {R_1}^2}}\right)} = 261\ kN$$

$$P_{max.LGH.Ø250} = m_{Rd} \cdot \frac{2\pi}{\left(1 - \sqrt[3]{\frac{{D_{Ø250}}^2}{4 \cdot {R_1}^2}}\right)} = 291\ kN$$

3.1.4 Numerical comparison

Theoretical load capacities calculated in sections 3.1.2 and 3.1.3 will be compared with the mean values of collected capacity tabled in section 2.2.2.

Ø150			
Theory	Theoretical capacity	Collected capacity	Utilization*
K.W.J.	207 kN	364 kN	176 %
L.G.H.	261 kN	364 kN	140 %

(a)

Ø250			
Theory	Theoretical capacity	Collected capacity	Utilization*
K.W.J.	207 kN	422 kN	204 %
L.G.H.	291 kN	422 kN	145 %

(b)

Figure 16 - Numerical comparison of theoretical and experimental data
a) Ø150 b) Ø250

** Utilization is calculated as the ratio of experimental data to theorical data.*

Both theories demonstrate a remaining capacity with L.G Hagsten [1] being closest to the collected data. Furthermore, it is worth noting that L.G. Hagsten [1] accounts for the column's extension, for which the theoretically derived influence appears to align with the collected data. This will be examined in greater detail.

The increase of capacity going from Ø150 to Ø250 as the only variable is compared between L.G. Hagsten [1] and tested data.

L.G.H: $\frac{(291\ kN - 261\ kN)}{261\ kN} = 12\ \%$

Test: $\frac{(422\ kN - 364\ kN)}{364\ kN} = 16\ \%$

The theory and practice have been observed to behave very similarly. Thus, the experiments confirm the assumption regarding the influence of the distributed plate derived in [1].

3.2 Crack behavior

Cracks have been observed to form radially starting from the center moving outwards. In some areas, these cracks are located directly beneath the reinforcement, which is believed to be due to notch effects.

Except for local conditions at the center, all cracks are seen to be radial. Furthermore, the radial crack pattern confirms that there is not a sufficiently large moment along the edges that needs to be accounted for. This observation is consistent with the theory proposed by Lars German Hagsten [1], where the bending moment decreases towards the edge of the foundation.

3.3 Verifying that punching shear is not critical

As demonstrated by the following calculations, punching shear is not critical.

The capacity is calculated in accordance with [2] section 6.4 and for the most critical static system: a pocket with a diameter of 1150 mm, as this is the largest measured pocket size, and for specimen group Ø250, as the control perimeter will be greatest as well as the load P = 423 kN (see Figure 15).

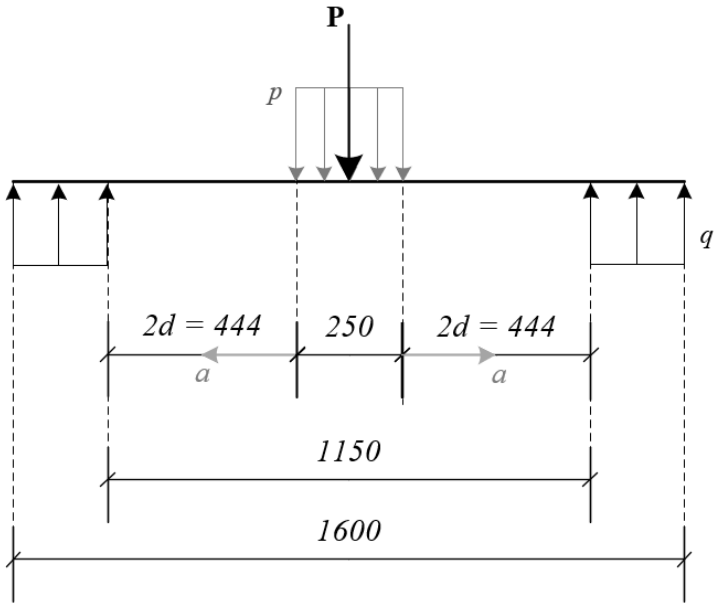

Figure 17 - Static system of specimen Ø250

Parameters for the foundation is as described in section 1.2.2. Strength parameters follow mean values given by [2] Table 3.1, f_{cm} = 53 MPa, and table C.1, f_t = 594 MPa. Both are calculated with a partial factor γ_i = 1,0.

		k		1,95 -	
		$C_{Rd,c}$		0,18 -	
Reinforcement ratio		ρ_{ly} / ρ_{lz}		0,0011 -	
Strength reduction factor		ν_v		0,45 -	
Distance coloumn edge	a	0 (0d)	444 (critical)	444 (2d)	mm
Controlperimeter	u	1000	3790	3790	mm
Punching shear	v_{Ed}	1,91	0,503	0,503	MPa
	V_{Ed}	423	423	423	kN
Punching shear capacity	$v_{Rd,c}$	11,93	1,010	1,010	MPa
	V_{Rd}	2647	850	850	kN
Utilization	U	16%	**50%**	50%	OK!

Figure 18 - Calculation, punching shear according to [2] section 6.4

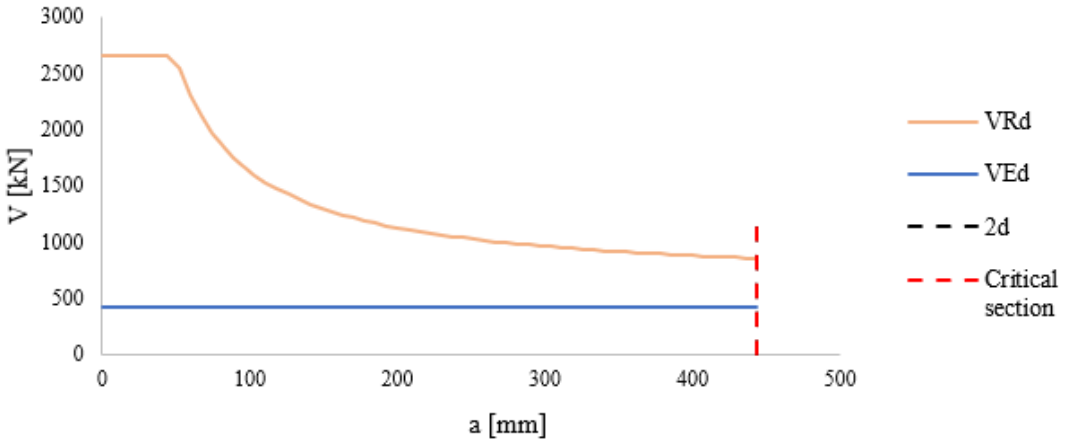

Figure 19 - Vizualisation, punching shear capacity and load
Graph going from the edge of the distributed area a = 0 mm to a = 2d = 444 mm

The calculation above shows that the foundation is only utilized by 50% for punching shear verifying that this is not critical.

3.4 Support conditions

The experiment has raised additional questions on the support conditions of the foundations. Theories for foundations assume a uniformly distributed surface load, but this is not expected to reflect reality. The following proposal suggests how the load might be distributed. This could potentially have a significant impact on the foundation's capacity, both in terms of shear and bending moment, and may explain why a considerable residual capacity is observed in the foundations.

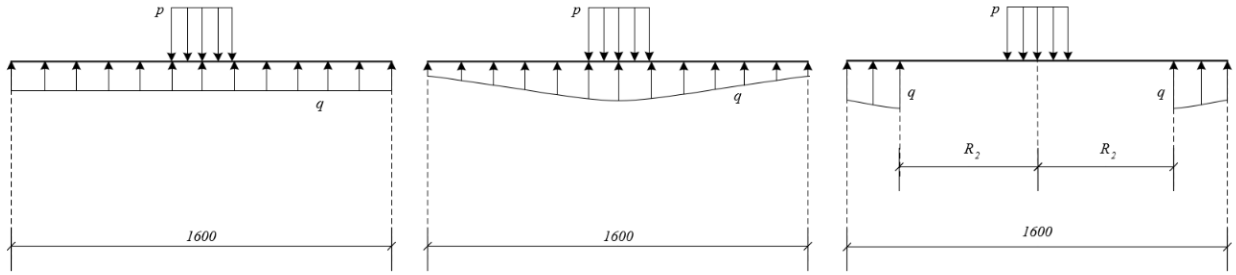

Figure 20 – Reactions
a) Assumption b) Possible reality c) With pocket

Conclusion

This study experimentally investigated six circular point foundations designed below the minimum reinforcement as specified in [2]. A ductile failure was still seen. It was ensured that the specimens would reach failure with bending moment being critical.

The tests confirm that the bending moment capacity increases as the distributed load area expands. This observation aligns with the exact solution for point foundations derived by Lars German Hagsten [1]. Further examination of the theory reveals that the increase in capacity derived theoretically and measured experimentally is 12% and 16%, respectively, when comparing the smaller to the larger distributed load diameter, with a ratio of 150/250.

Additionally, the study includes experimental data indicating that upward-bent reinforcement along the edges is not necessary. No cracks have been observed parallel to the edge that would suggest a moment in this direction. This observation further corroborates Lars German Hagsten's theory [1], where the bending moment approaches zero at the foundation's edge.

Finally, it has been observed that residual capacity exists in the foundation according to both K.W.J [3][4] and L.G.H. [1]. It is discussed whether the support conditions could significantly influence this residual capacity.

Acknowledgement

We would like to express our gratitude to the Department of Civil Engineering at Aarhus University for providing the facilities and resources essential for conducting the experiments. We also appreciate the valuable input from the dedicated professors at Aarhus University. Furthermore, we are grateful to Industri Beton A/S for their collaboration and for producing the custom-designed foundations used in the experiments. Finally, we extend our thanks to Value Engineering ApS for their theoretical guidance and financial support.

Appendix A

Below the upper bound solution of a foundation supported by a uniformly distributed load is presented following [1].

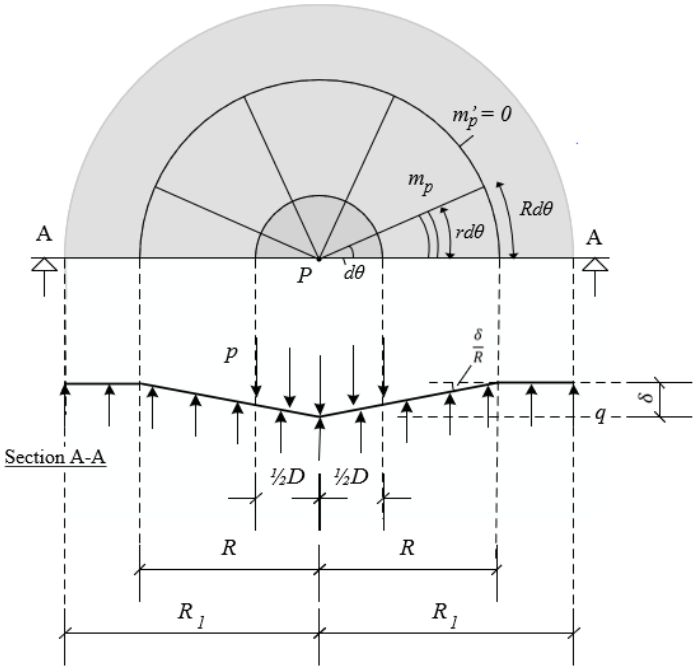

External work:

$$A_o = P \cdot \delta - \int_0^R \int_0^{2\pi} \frac{R-r}{R} \delta \cdot q \cdot r d\theta \cdot dr$$

Internal work:

$$A_i = \int_0^R \int_0^{2\pi} m_p \cdot dv \cdot dr$$

Extension of *R* that shapes the most critical failure mechanism:

$$R = \sqrt[3]{\frac{1}{2} \cdot D \cdot {R_1}^2}$$

In the following the pocket's extension, R_2, is considered. The outer shaded area represents where the reaction under the foundation acts, while the inner, non-shaded area, represents the extension of the pocket.

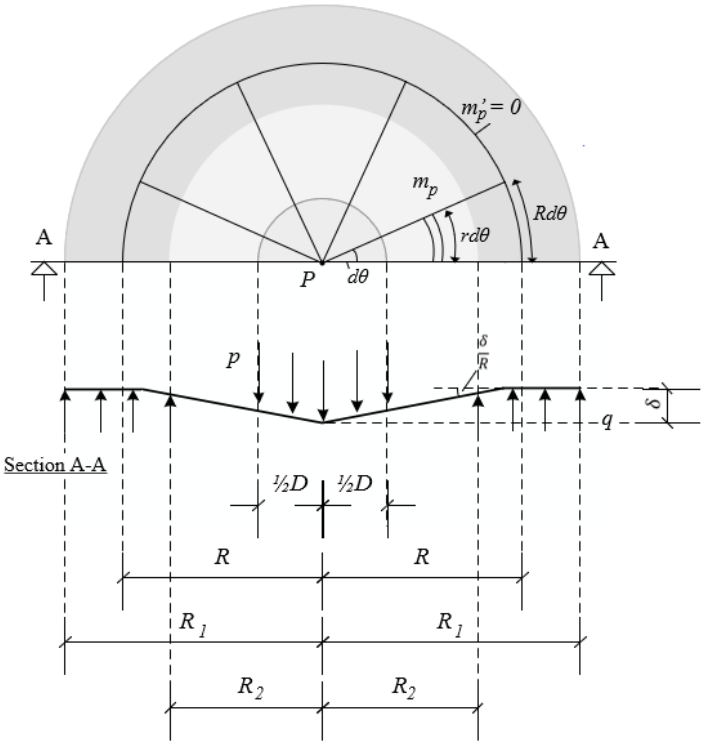

External work:

$$A_{o.pock} = \int_0^{½D} \int_0^{2\pi} \frac{R-r}{R} \delta \cdot q \cdot rd\theta \cdot dr - \int_{R_2}^{R} \int_0^{2\pi} \frac{R-r}{R} \delta \cdot p \cdot rd\theta \cdot dr$$

Internal work:

$$A_{i.pock} = \int_0^R \int_0^{2\pi} m_p \cdot dv \cdot dr$$

Extension of *R* that shapes the most critical failure mechanism:

$$R_{.pock} = \sqrt[3]{\frac{D \cdot {R_1}^2 + 2 \cdot {R_2}^3 - D \cdot {R_2}^2}{2}} \ ,$$

$$\text{As } q = \frac{P}{2\pi} \cdot \frac{8}{D^2} \text{ and } p = \frac{P}{2\pi} \cdot \frac{2}{({R_1}^2 - {R_2}^2)}$$

The two failure mechanisms will be compared for their solution of the equation for $A_i = A_o$, solving for the bending moment, m_p:

Without pocket

$$m_p = \frac{P}{2\pi} \cdot \frac{1}{3} \cdot \left(3 - \frac{D}{R}\right) - \frac{1}{3} \cdot \frac{R^2}{{R_1}^2}$$

With pocket

$$m_{p.pock} = \frac{P}{2\pi} \cdot \frac{1}{3} \cdot \frac{\left(R^3 - 3 \cdot {R_1}^2 \cdot R + ({R_1}^2 - {R_2}^2) \cdot D + 2 \cdot {R_2}^3\right)}{R \cdot (R_2 - R_1) \cdot (R_2 + R_1)}$$

The increment of the load, *P*, due to the pocket R_2 is described by:

$$k = \frac{m_{p.pock}}{m_p}$$

References

[1] Lars German Hagsten. *"Point Foundation. Lower Bound Solution for Distributed Load"*. Proceedings of the Danish Society for Structural Science and Engineering. No. 1, May 2023, page 1-6.

[2] DS/EN 1992-1-1 + AC:2008

[3] K.W. Johansen. *"Brudlinieteorier [Yield line theories]"* 1943.

[4] K.W. Johansen. *"Yield line theory"* Cement and Concrete Association. 1962.

[5] Dansk Ingeniørforening. *Teknisk Ståbi* (26. udg.) Polyteknisk Forlag. 2018.

[6] International Energy Agency (IEA) & United Nations Environment Programme (UNEP). *"2019 Global Status Report for Buildings and Construction: Towards a zero-emission, efficient and resilient buildings and construction sector."* 2019.

[7] MTS DuraGlide 201 Hydraulic Actuators. Product specification used for this experiment: MTS 201.35G2..

Danish Society for Structural Science and Engineering

Requests for membership of the society are submitted to one of the board members:

The purpose of the society is to work for the scientific development of structural mechanics - both theory and construction of all kinds of load-bearing structures - promote interest in the subject, work for a collegial relationship between its practitioners and assert its importance to and in collaboration with other branches of engineering. The purpose is sought realized through meetings with lectures and discussions as well as through the publication of the Proceedings of the Danish Society for Structural Science and Engineering.

Individual members, companies and institutions that are particularly interested in structural mechanics or whose company falls within the field of structural mechanics can be admitted as members.